

# Bond of RC members using nonlinear 3D FE analysis

S. Lettow, J. Özbolt & R. Eligehausen

*Institute of Construction Materials, University of Stuttgart, Germany*

U. Mayer

*nolasoft - design office, Stuttgart, Germany*

**ABSTRACT:** Behaviour of reinforced concrete depends on the transfer of tensile forces from reinforcing bars into concrete. This transfer relies on the bond. Therefore, in the finite element modelling of RC members one needs a simple and realistic bond model. In the present paper a discrete bond model which is used in the three-dimensional finite element analysis of RC structures is described and its performance is demonstrated on a few numerical examples. The numerical results are compared with the experimental results.

**Keywords:** reinforced concrete, bond, discrete bond element, bond model, nonlinear finite element analysis

## 1 INTRODUCTION

In the past a number of experimental investigations have been carried out in order to clarify and understand the behaviour of deformed bars pulled out from a concrete block under monotonic and cyclic loading conditions. These experimental results are well documented in the specific literature (e.g. CEB Bulletin No. 230 1996, fib Bulletin No. 10 2000). Based only on the experimental results it is difficult to filter out the influences of material and geometrical parameters on the bond behaviour. Therefore, to better understand the bond behaviour, a reliable bond model (interaction between reinforcing bars and concrete) that can be employed in a three-dimensional finite element analysis is needed. The numerical modeling of the bond behaviour is principally possible at two different levels: (1) phenomenological modeling based on a smeared or discrete formulation of the bar-concrete interface and (2) detailed analysis in which the geometry of the bar and the concrete is modeled by three-dimensional elements. In this case the model is formulated in the framework of continuum or of discrete type modeling (e.g. lattice model, random particle model, etc.).

In the phenomenological modeling of bond the concrete and the reinforcing bars are discretised by two- or three-dimensional finite elements. The link between the bar and the concrete can be realised either by a continuous or discontinuous connection. In the continuous connection the macroscopic stress-strain constitutive relationship has to be employed whereas in the discontinuous approach bond is defined by discrete, zero-thickness elements (springs) whose behaviour is controlled by the stress-slip relationship. Both approaches are able to realistically predict the bond behaviour for different geometries and for different boundary conditions only if a realistic constitutive model for the surrounding concrete is used. However, these models are not able to automatically predict the bond behaviour of a given bar geometry. For instance, it is not possible to predict the influence of the geometry of the ribs as well as the influence of their spacing on the bond behaviour. Consequently, the influence of these parameters must be stored in advance in the basic parameters of the bond model. Furthermore, in case of the continuous approach the finite element mesh has to be relatively fine which leads, especially in complex structures, to a long “meshing process” and to an increase of the computing time.

Using adequate discrete bond elements, which describe the interaction between reinforcement and concrete, the efficiency and the accuracy of numerical investigations of the load bearing behaviour of reinforced concrete members can be increased in most practical applications.

## 2 DISCRETE BOND ELEMENT

### 2.1 General concept

The bond element which is implemented in a three-dimensional finite element code (MASA "microplane model" for concrete, see Ožbolt et al. 2001) and used in the following examples connects a steel reinforcing bar (truss or bar finite element) with the surrounding concrete that is discretised by the three-dimensional finite elements. Only the degrees of freedom in the bar direction (slip) are considered. The connection to concrete perpendicular to the bar direction is assumed to be perfect. When a ribbed bar is pulled out from a concrete block, besides the stresses parallel to the bar direction (tangential shear stresses), the stresses perpendicular to the bar direction (radial stress) are generated as well. For a given slip the radial stresses depend on the geometry of the bar (rib height and rib spacing) as well as on the geometry of the concrete specimen (bar close to or far from the edge, confining reinforcement, etc.). In the proposed model it is assumed that the radial stresses are generated by the concrete finite elements. The interaction between shear and radial stresses is accounted for in two different ways: (1) directly, with the shear stresses related to the nonlocal (representative) radial stresses obtained from the concrete elements close to the reinforcing bar and (2) indirectly, with the larger shear stresses (e.g. higher bond strength due to larger ribs) caused by a higher activation of the stresses in the radial direction.

### 2.2 Model response under monotonic and cyclic loading

The experimental evidence (CEB Bulletin 230 1996, fib Bulletin No. 10 2000) indicates that the load transfer between reinforcement and concrete is mainly accomplished through bearing of the reinforcing bar lugs on the surrounding concrete and through friction at large slip values. The adhesion is negligible. This behaviour can be described using so-called bond stress-slip relationships. The total bond resistance can be decomposed into two components: (1) the

mechanical interaction component  $\tau_m$  and (2) the frictional component  $\tau_f$ . The frictional component can be separated into a residual friction  $\tau_r$  and a virgin friction  $\tau_v$ . The residual friction represents frictional resistance upon slip reversal whereas the virgin friction component is due to the additional frictional resistance developed upon loading to previously undeveloped slip levels. The bond stress-slip relationship which is used in the model and the corresponding components are shown in Figure 1.

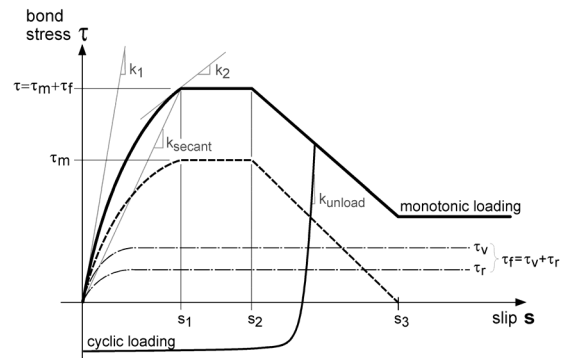


Figure 1. Bond stress-slip relationship of the bond element model.

Based on experimental results (see for instance Elgehausen et al. 1983, Lowes et al. 2001) the bond stress-slip relationship can be described by the parameters that are summarised in Table 1.

Table 1. Summary of the model parameters.

Description of the model parameter	Model parameter	Units
peak mechanical bond strength	$\tau_m = \tau_{m,0} \Omega^m$	[N/mm <sup>2</sup> ]
peak frictional bond strength	$\tau_f = \tau_{f,0} \Omega^f$	[N/mm <sup>2</sup> ]
secant to bond response curve for initial loading	$k_{secant}$	N/mm <sup>2</sup> /mm]
slip at which peak bond strength is achieved	$s_1 = (\tau_m + \tau_f)/k_{sec}$	[mm]
slip at which bond strength begins to decrease	$s_2$	[mm]
slip at which mechanical bond resistance is lost	$s_3$	[mm]
tangent to the load-displacement curve upon unloading	$k_{unload}$	[N/mm <sup>2</sup> /mm]

The parameters  $\tau_{m,0}$  and  $\tau_{f,0}$  represent the strength of the mechanical and frictional component (subscript m and f), respectively, for the case of no confining pressure, no damage and elastic reinforcing steel. The factor  $\Omega^i$  takes into account

the boundary conditions which influence the particular bond strengths and  $\Omega^i$  is obtained by multiplying the single influencing factors ( $\Omega^i = \Omega_s \Omega_c \Omega_{cyc}$ ). Thereby the factor  $\Omega_s$  accounts for the strain state in the reinforcing bar,  $\Omega_c$  considers the state of stress in the surrounding concrete and  $\Omega_{cyc}$  rules the influence of loading, unloading and reloading on the bond behaviour.

### 2.3 Implementation of the bond element

The model used in the finite element code defines bond strength and stiffness as a function of the relative displacement (slip) between concrete and reinforcing steel. The model is incorporated into a finite-length and zero-width bond element for the use in the three-dimensional finite element analysis of reinforced concrete structures (see Fig. 2). It connects the truss finite element (reinforcing bar) with a three-dimensional concrete solid finite element. To determine the transmissible bond force only the slip in the bar direction is considered. A sketch of the bond element and the element displacement field is given in Figure 2.

A more detailed description of the bond model is given in Ožbolt et al. (2002).

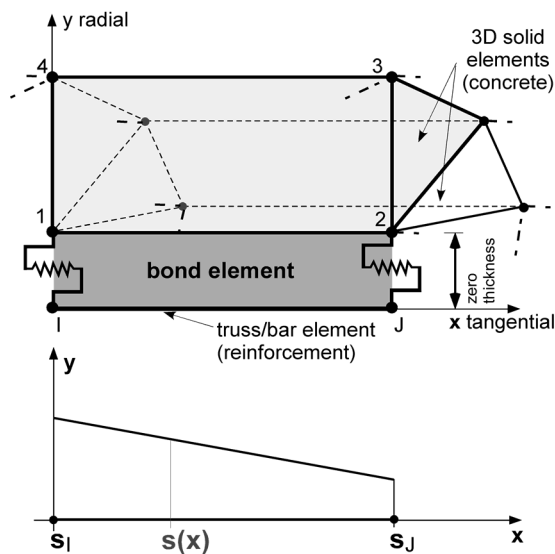


Figure 2. Schematic bond element and element displacement field.

## 3 NUMERICAL AND EXPERIMENTAL INVESTIGATIONS

### 3.1 Pull out tests with a short embedment length

To investigate the performance of the bond elements and to calibrate the parameters of the basic model, calculations on pull-out tests (so-called "ringtest") of a reinforcing bar ( $d_s = 12$  mm) embedded in concrete (embedment length  $l_E = 60$  mm) surrounded by a steel ring ( $d_R = 60$  mm) have been carried out. The results of these numerical investigations are compared with the results of the experimental investigations (Lettow et al. 2003). The test-setup is shown in Figure 3.

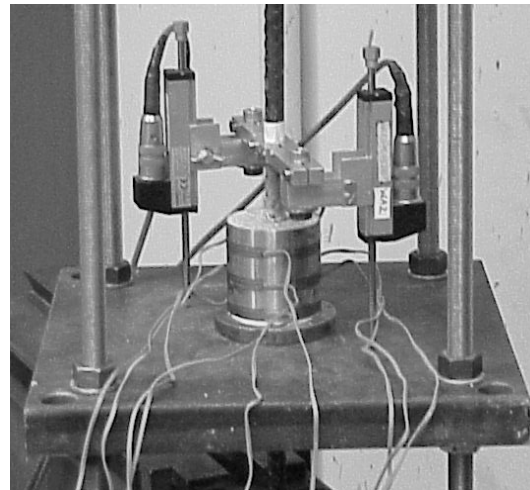


Figure 3. Test setup: pullout tests with a short embedment length.

In the experimental investigations beside the force and the unloaded end displacement, the tensile (hoop) strains in the steel ring at different locations have been measured using strain gauges. These results are used to obtain information on the distribution of the splitting forces along the embedment length. The calculations were performed using a finite element model with (one-dimensional) bar elements to represent the reinforcement, solid elements for concrete and discrete bond elements for the simulation of the bond behaviour. Figure 4 shows the finite element mesh. To get realistic results the average size of the concrete elements close to the bar elements has to be 1.2 times the bar diameter (Ožbolt et al. 2002).

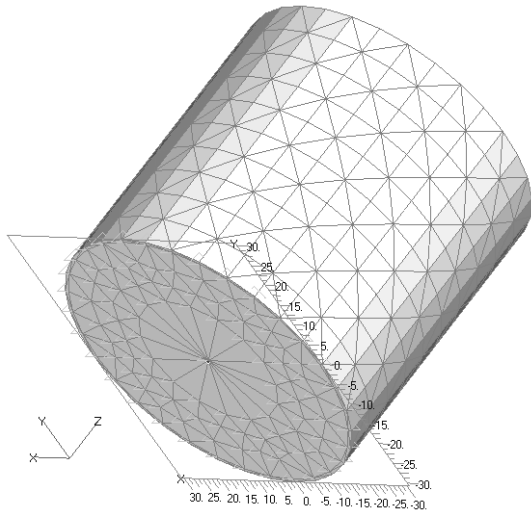


Figure 4. Finite element mesh: pullout test with a short embedment length.

In Figure 5 both the measured and the calculated average bond stresses are shown as a function of the relative displacement at unloaded end (slip). In Figure 6 the hoop strains in the steel ring (measured and calculated values) are plotted over the slip at unloaded end.

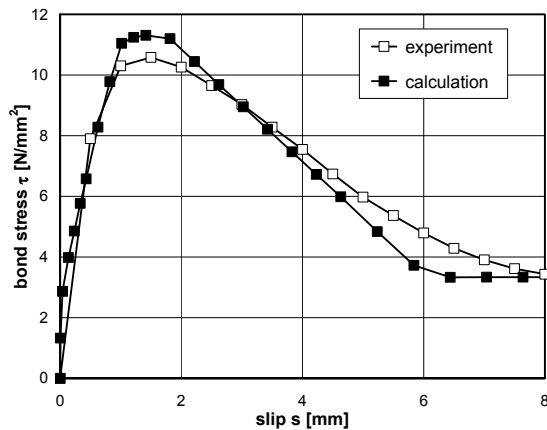


Figure 5. Measured and calculated average bond stresses as a function of the slip at unloaded end.

By the use of adequate parameters in the basic bond model the shape of the calculated bond stress-slip curve agrees very well with the measured curve. Especially the measured bond strength, the measured bond stiffness and the corresponding slip values (at bond strength and friction) are simulated very well. A good agreement between tests and calculations can also be seen from Figure 6, which

shows the distribution of the hoop strains as a function of the slip.

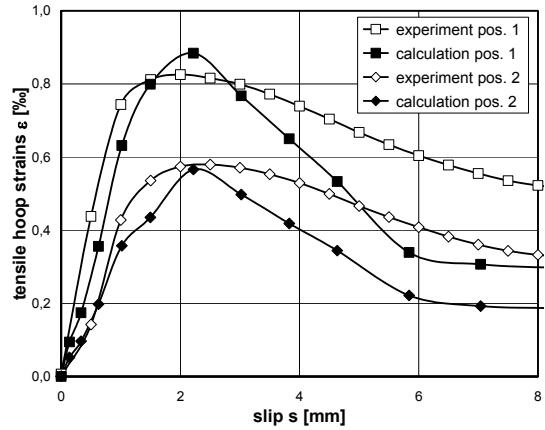


Figure 6. Measured and calculated hoop strains in the steel ring as a function of the slip at unloaded end.

The results of an additional calculation without the surrounding steel ring are shown in Figure 7. The bond stress-slip curve of the first calculation (with surrounding steel ring) is shown as well. While in the first calculation the failure takes place by pull out of the bar, due the confinement of the steel ring, in the additional calculation splitting failure occurs. This can be recognised in the bond stress-slip curves as well. With splitting of the concrete the bond strength is significantly reduced. In Figure 8 the crack pattern by means of principal tensile strains is shown. This example shows the capability of the model to simulate both "bond failure modes".

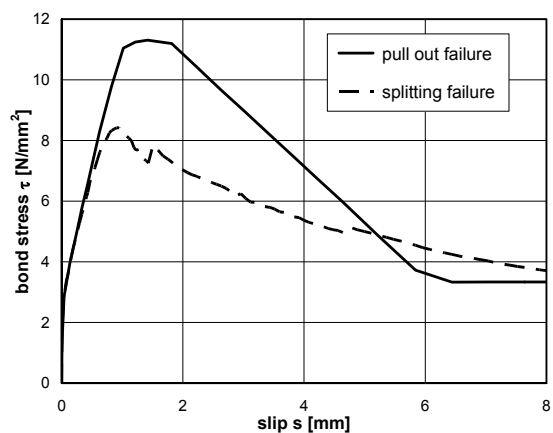


Figure 7. Calculated average bond stresses as a function of the slip at unloaded end (calculations with and without steel ring).

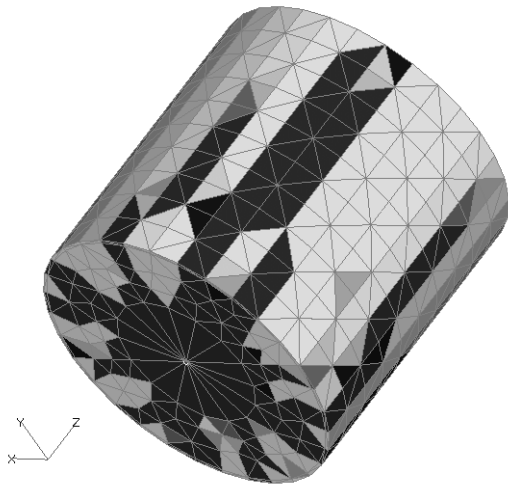


Figure 8. Crack pattern (splitting) by means of principal tensile strains (calculation without steel ring).

### 3.2 Pullout tests with a long embedment length

The bond behaviour of ribbed reinforcement was investigated by Shima et al. (1987) in a large number of experimental and theoretical studies. To determine the influence of the steel strain in the bar the embedment length in the pullout tests was chosen such that the yield force of the bar was reached and exceeded, respectively ( $l_E = 40 d_s$ ). Longitudinal cracking or splitting of the specimen was avoided by a sufficiently large concrete cover. Furthermore, to prevent an influence of the free surface on the bond behaviour (local cone failure) at the loaded end the bar had an unbonded length of  $10 d_s$ . The steel strains were measured with strain gauges, which were placed along the bar on the opposite sides. The relative displacement at the unloaded end between concrete and steel bar (slip) was recorded by LVDTs.

To demonstrate the influence of inelastic steel strains and transverse contraction (Poisson-effect), respectively, bars with highly different shapes of the stress-strain diagram were tested (see Fig. 9). The concrete uniaxial compressive strength was  $f_c' = 19.6 \text{ N/mm}^2$ . The test setup (schematic) is shown in Figure 10.

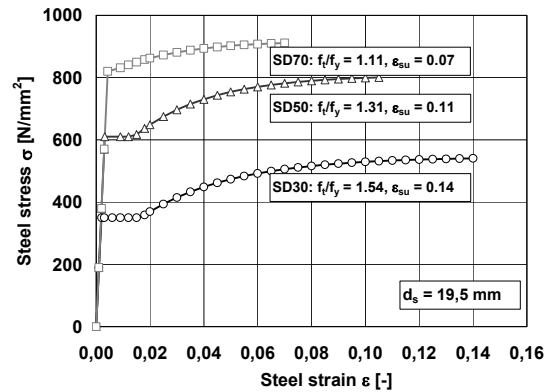


Figure 9. Steel stress-strain diagrams used in experiments and calculations.

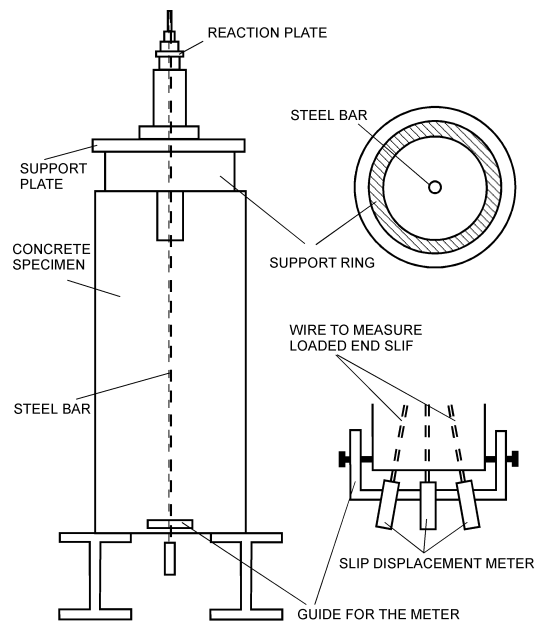


Figure 10. Test setup: pullout tests with a long embedment length (after Shima et al. 1987).

The finite element mesh used in the calculations is given in Figure 11. The reinforcement was modeled with bar elements. These elements were linked to the solid elements, which represent the concrete, using the above described discrete bond elements.

The tests and the calculations were performed for the steel stress-strain diagrams plotted in Figure 9.

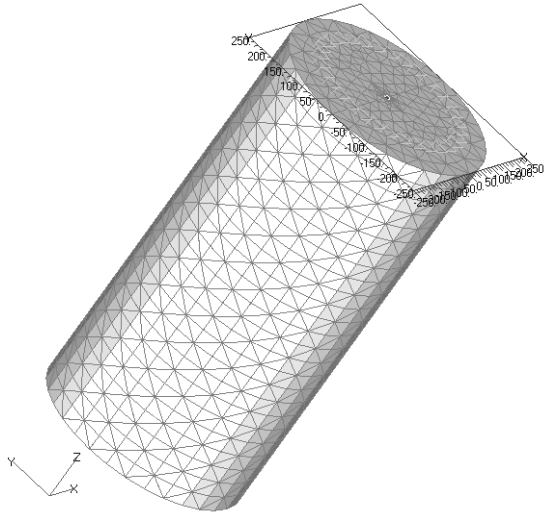
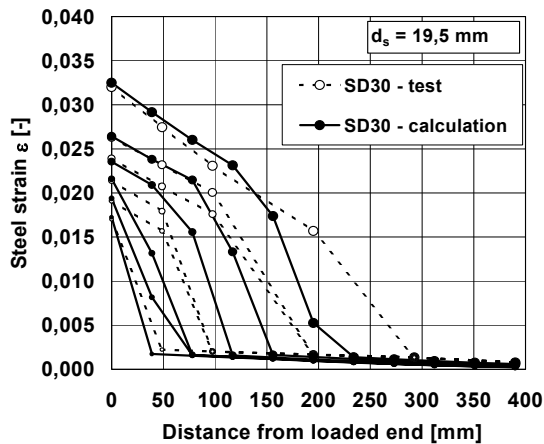
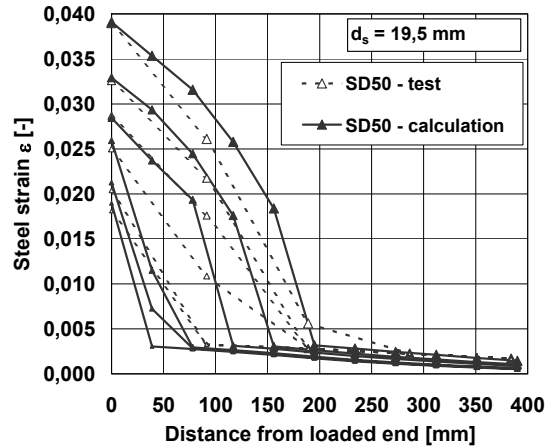


Figure 11. Finite element mesh: pullout-tests with a long embedment length.

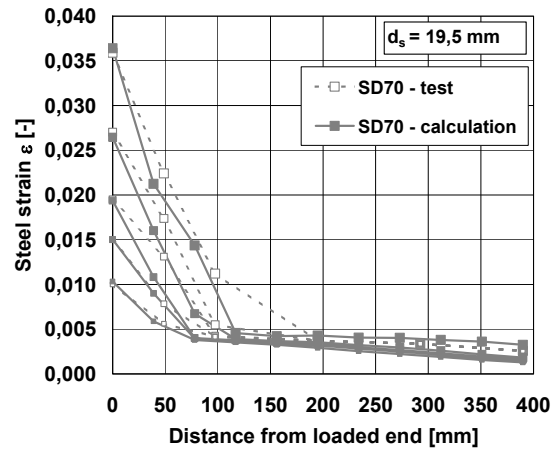
The comparison between the measured and the calculated distribution of steel strains for the different steel stress-strain diagrams along the embedment length is shown in Figures 12a, b, c. The curves show the expected shape, i. e. with increase of the distance from the loaded end the inelastic steel strain decreases. It can be seen that the strain gradient is significantly influenced by the shape of the steel stress-strain diagram. From the measured and calculated curves it is obvious that the agreement is rather good. This means that the influence of inelastic steel strains on the bond behaviour is correctly simulated by the used bond model. Moreover a good agreement between tests and calculations was found for the distribution of the bond stresses and displacements.



a. Results obtained using stress-strain diagram: SD30.



b. Results obtained using stress-strain diagram: SD50.



c. Results obtained using stress-strain diagram: SD70.

Figure 12. Inelastic steel strains at different load levels as a function of the distance from the loaded end.

### 3.3 Tension tests on RC columns

The stiffness of tension members with a square cross-section loaded up to rupture of the reinforcement was investigated in a series of 34 tests. The tests were carried out with varying reinforcement percentage  $\rho$ , bar diameter  $d_s$ , steel ductility (ductility classes B, A and S according to CEB-FIP Model Code 90 1993) and concrete strength. The aim of the study was to investigate the contribution of concrete between cracks (tension stiffening) beyond yielding of the reinforcement. For more details see Eligehausen et al. (2003).

To validate the bond model elements concerning the crack formation (crack width and crack spacing)

as well as the influence of inelastic steel strains on the tension stiffening effect a few tests were simulated. In the following the measured and calculated results of one test (4 bars  $d_s = 16$  mm with strain gauges applied on the surface, hot rolled steel with a distinct yield plateau  $f_t/f_y = 1.13$  and  $\epsilon_{su} = 0.0875$ , square cross-section 400 x 400 mm, concrete  $f_{cc} = 25.0$  N/mm<sup>2</sup>) are presented. In the calculation model a double-symmetry was used. During the tests the force and the overall elongation as well as the crack width (on each specimen side) was measured. The test setup is shown in Figure 13. Figure 14 shows the finite element mesh used in the calculation.

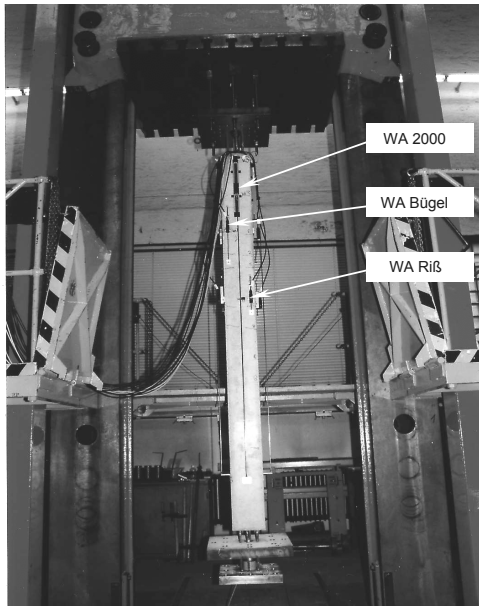


Figure 13. Test setup of tension tests.

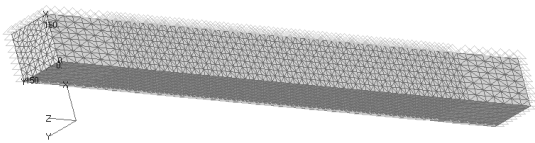


Figure 14. Finite element mesh: Tension tests on RC members.

Using the principal tensile strains the cracks and therefore the crack spacing (after completed crack formation) can be obtained. Figure 15 shows the crack pattern according to the test and the calculation. The measured mean crack spacing is in average about 300 mm, in the calculation the average distance between the cracks is approximately 280 mm.

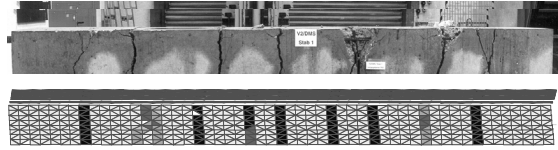


Figure 15. Crack spacing according to experiment and calculation.

The localisation of steel strains at the cracks and the reduction of the steel strain between two cracks (contribution of concrete) is clearly visible from Figure 16.

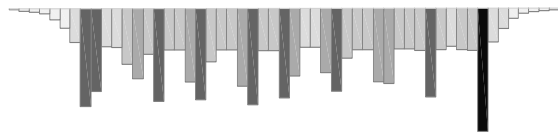


Figure 16. Steel strain in the reinforcing bar.

To display the overall load-deformation property of a tension member, especially for inelastic steel strains, diagrams which show the ratio between average steel strain  $\epsilon_{sm}$  and steel strain at the crack  $\epsilon_{sr}$  as a function of the steel strain at the crack  $\epsilon_{sr}$  are useful. A small ratio  $\epsilon_{sm}/\epsilon_{sr}$  means a large contribution of concrete and a ratio  $\epsilon_{sm}/\epsilon_{sr} = 1$  means bare bar response. The measured and calculated ratios  $\epsilon_{sm}/\epsilon_{sr}$  as a function of  $\epsilon_{sr}$  are shown in Figure 17. As can be seen, the agreement between experimental and numerical results over the entire steel strain range is rather good.

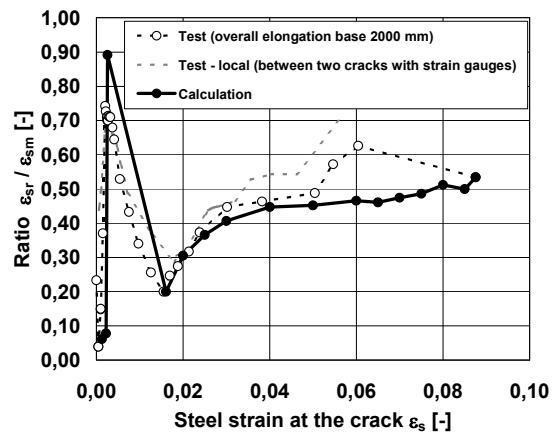


Figure 17. Measured and calculated ratios between average steel strain  $\epsilon_{sm}$  and steel strain at the crack  $\epsilon_{sr}$  as a function of the steel strain at the crack  $\epsilon_{sr}$ .

## 4 CONCLUSIONS

A new zero-thickness bond element that is based on the proposed bond stress-slip relationship is implemented into a three-dimensional finite element code. The bond element accounts for the influence of the reinforcement strains, the influence of the stress state of the surrounding concrete as well as for the influence of the cyclic loading history on the bond response. It is assumed that the radial stresses are generated by the surrounding concrete finite elements. The interaction between tangential and radial stresses is accounted for in two different ways: (1) directly, with the shear stresses related to the nonlocal (representative) radial stresses obtained from the concrete elements close to the reinforcing bar and (2) indirectly, with the larger shear stresses (e.g. higher bond strength due to larger ribs) caused by a higher activation of the stresses in the radial direction.

The model is incorporated into a finite-length and zero-width bond element. The bond element is a two-node finite element and it connects a truss/bar finite element (reinforcement) with a three-dimensional solid finite element (concrete). The element displacement field is a slip, which is defined as the relative displacement between the reinforcing bar and the concrete in the direction of the reinforcing bar.

To check the potential and the accuracy of the model, several finite element calculations have been carried out by varying the input parameters of the bond model. This was performed using different finite element models to study and compare the 'global' and 'local' response and to investigate different failure modes, i.e. to see whether the model is able to distinguish between pull-out and splitting failure mode. The finite element studies of pullout tests with a short and a long embedment length and tests on tension members show a good agreement between experimental and numerical results. The new discrete bond element is able to predict transfer of bond stresses from reinforcement into concrete realistically. This holds especially for large reinforcement strains, where yielding of the steel occurs.

To further test and improve the model and to calibrate its input parameters, more finite element studies for cases in which the bond plays a decisive role have to be carried out in the future.

## 5 REFERENCES

- CEB Bulletin d'Information No. 213/214 1993. CEB-FIP Model Code 1990. London: Thomas Telford Ltd.
- CEB Bulletin d'Information No. 230 1996. RC elements under cyclic loading. State of the art report. London: Thomas Telford Ltd.
- Eligehausen, R., Popov, E.P. & Bertero, V.V. 1983. Local bond stress-slip relationships of deformed bars under generalized excitations. Report No. UCB/EERC-83/23. University of California Berkeley: Earthquake Engineering Research Center.
- Eligehausen, R., Mayer, U. & Lettow, S. 2003. Mitwirkung des Betons zwischen den Rissen in Stahlbetonbauteilen (contribution of concrete between cracks in RC members). Abschlussbericht zum DFG-Forschungsvorhaben EL 72/8-1 + 2: Mitwirkung des Betons zwischen den Rissen nach Erreichen der Fließgrenzen der Bewehrungen in Spannbeton- und Stahlbetontragwerken. Universität Stuttgart: Institut für Werkstoffe im Bauwesen.
- fib-Bulletin No. 10 2000. Bond of reinforcement in concrete – state-of-the-art report, Lausanne: fédération internationale du béton.
- Lettow, S., Mayer, U. & Eligehausen, R. 2003. Experimentelle Untersuchungen zum Verbundverhalten von gerippten Bewehrungsstäben (experimental investigations on the bond behaviour of ribbed reinforcing bars). Universität Stuttgart: Institut für Werkstoffe im Bauwesen.
- Lowes, N.L., Moehle, J.P. & Govindjee, S. 2002. A concrete-steel bond model for use in finite element modeling of reinforced concrete structures. To be published in the ACI Special Publication.
- Ožbolt, J., Li, Y.-J. & Kožar, I. 2001. Microplane model for concrete with relaxed kinematic constraint. *International Journal of Solids and Structures*. 38: pp. 2683-2711.
- Ožbolt, J., Lettow, S., & Kožar, I. 2002. Discrete Bond Element for 3D Finite Element Analysis of Reinforced Concrete Structures. In Balázs-Bartos-Cairns-Borosnyói (eds), Proceedings of the 3rd International Symposium: Bond in Concrete - from research to standards. Budapest: University of Technology and Economics.
- Shima, H., Chou, L.-L. & Okamura, H. 1987. Micro and macro models for bond in reinforced concrete. *Journal of the Faculty of Engineering*. Vol. XXXIX, No. 2. The University of Tokyo.